Journal of Inflammation Research Dovepress

Open Access Full Text Article ORIGINAL RESEARCH

Jiawei Qifuyin Enhances Immunity and Improves Cognitive Impairment in APP/PS1 Mice Through Modulation of Neuroinflammatory Pathways

Jiahua Cheng[1,*], Wujuan Li[1,*], Lanlin Wang[1,*], Yu Gao[1], Yueran Ma[1], Min Zhou[1], Tian Yang[1], Changwu Yue[1,2], Long Yan[3], Yuhong Lyu[1,2]

[1]Yan'an Key Laboratory of Microbial Drug Innovation and Transformation, School of Basic Medicine, Yan'an University, Yan'an, Shaanxi, People's Republic of China; [2]Shaanxi Engineering and Technological Research Center for Conversation and Utilization of Regional Biological Resources, Yan'an University, Yan'an, Shaanxi, People's Republic of China; [3]Medical Imaging Center, Yan'an Traditional Chinese Medicine Hospital, Yan'an, Shaanxi, People's Republic of China

*These authors contributed equally to this work

Correspondence: Long Yan; Yuhong Lyu, Email yanlong840212@163.com; yuhonglyu@126.com

Purpose: To explore the protective effects and mechanisms of Jiawei Qifuyin on APP/PS1 mice, a model for Alzheimer's disease (AD).

Methods: Network pharmacology tools were used to predict anti-AD targets and signaling pathways affected by Jiawei Qifuyin. In vitro studies assessed antioxidant and oxygen radical scavenging abilities, immune cell proliferation, and inflammatory cytokine levels in lipopolysaccharide-induced BV2 microglial cells. Cognitive ability in APP/PS1 mice was evaluated using the Morris Water Maze test. mRNA expression of neuroinflammatory factors, changes in intestinal microbiota, and short-chain fatty acid content were analyzed post-treatment.

Results: Network pharmacology predicted that Jiawei Qifuyin affects AKT1, TNF-α, and AGE/RAGE pathways. It showed concentration-dependent antioxidant effects and modulated immune cell proliferation. IL-2, IL-6, and TNF-α levels in LPS-induced BV2 cells were significantly reduced. Treated animals exhibited improved cognitive performance, decreased brain amyloid-beta levels, and downregulated expression of IL-1β, IL-6, RAGE, and NF-κB. Significant changes in intestinal microbiota composition and SCFA content were observed.

Conclusion: Jiawei Qifuyin may enhance immunity and improve cognitive impairment in APP/PS1 mice through regulation of inflammatory factors, gut microbiota, and the gut-brain axis.

Keywords: Alzheimer's disease, Jiawei Qifuyin, neuroinflammation, intestinal microbiota, short chain fatty acid

Introduction

Alzheimer's disease (AD) is a central neurodegenerative disease, in which cognitive function gradually deteriorates with age. The pathological features mainly manifest in brain β-amyloid protein deposition, neuronal fiber entanglement, and central nervous system inflammation.[1,2] AD is a multifactor complex disorder, and currently, most treatments for AD are based on the cholinergic hypothesis, β-amyloid deposition hypothesis, tau protein hypothesis, and lysosomal acidification disorder hypothesis. With the gradual progress in research on AD, increasing evidence shows that the onset of AD is related to multiple factors, including family genetics, Aβ plaque-related neurodegeneration, neurofibrillary degeneration, synaptic dysfunction and neurotransmitter imbalance, neuroinflammation, infectious disease hypothesis, intestinal microbiota imbalance, gene mutations, oxidative stress, and autophagic lysosomal acidification. However, owing to the uncertainty and complexity of the pathogenesis of AD, the current progress in the treatment of AD is still very difficult.[3] Neuroinflammation is a defense response that occurs when brain tissues and cells are stimulated by disease-causing agents. Neuroinflammation is closely associated with microglia and astrocytes.[4] Stimulation of the brain with

Received: 20 June 2024
Accepted: 31 October 2024
Published: 18 November 2024

disease-causing factors causes the activation of these cells, which in turn produces inflammatory factors that damage the brain. However, the incidence of AD is still significantly increasing, causing a heavy burden on patients, their families, and society. Therefore, it is important and urgent to develop drugs that can reduce the incidence of AD and intervene in the development process of AD based on the pathological mechanisms of AD. The drugs used to treat AD clinically include donepezil, litramine, galantamine, memantine hydrochloride, and the new drug aducanumab, which were approved by the FDA in 2021. Although these drugs have achieved certain results in the treatment of AD, they do not fundamentally solve the problem of irreversible disease progression. Furthermore, many drugs have failed in clinical trials, forcing people to recognize the need to change the traditional development strategies for treating AD. The presence of amyloid proteins is insufficient to cause dementia. It is precisely because of the interaction between amyloid proteins and neuroinflammation that neurofibrillary tangles spread in the cortex, eventually leading to cognitive dysfunction in patients with AD. Therefore, neuroinflammation plays an important role in AD pathogenesis. Transient neuroinflammation is inflammation that carries out a restorative response to tissue cells and plays a protective role in nerves, leading to an inflammatory microenvironment that leads to tissue damage. Microglia are immune cells of the brain. In the early stages of AD, microglia are activated to phagocytose and remove amyloid deposits, thus achieving a neuroprotective effect. As the disease progresses, microglia change from an anti-inflammatory phenotype to a pro-inflammatory phenotype, secreting inflammatory factors, causing neuroinflammation, damaging neurons, damaging the brain, and aggravating cognitive impairment of patients.[5] Therefore, the regulation of neuroinflammation may be an important target for intervention in AD. Traditional Chinese medicine (TCM) has become a hot topic in the research of anti-AD drugs because of its advantages, such as low price, low toxicity, and obvious intervention effect on AD. Traditional Chinese medicine formulas are composed of a combination of multiple herbs that contain multiple active ingredients. Therefore, they can exert synergistic effects on AD intervention at the whole-body level by acting on multiple drug targets, pathways, and levels. Qifuyin, a traditional Chinese medicine prescription, is composed of seven traditional Chinese medicines: ginseng, prepared Rehmannia, Angelica, Atractylodes macrocephala, roasted licorice, wild jujube kernel, and Polygala tenuifolia. Modern pharmacological studies have found that it has a significant protective effect in animal models of Alzheimer's disease, stroke, and diabetes.

Based on a statistical analysis of 300 traditional Chinese medicine formulas for brain strengthening and intelligence enhancement, Jiawei Qifuyin-added Poria cocos to strengthen the spleen and calm the nerves; grass-leaved sweet flag Awakens Mind and Enlightens Wisdom, a new traditional Chinese medicine compound (ginseng 6 g, prepared Rehmannia 9 g, Angelic 9 g, Atractylodes macrocephala 5 g, prepared licorice 3 g, semen ziziphi spinosae 6 g, polygala tenuifolia 5 g, Poria cocos 12 g, grass-leaved sweet flag 8 g) was built.

This study first used network pharmacology to explore and predict the active components, targets, biological processes, and related signaling pathways of Jiawei Qifuyin in anti-AD.[6] We further investigated the biological activity of Jiawei Qifuyin using cellular experiments. Finally, animal experiments were conducted to explore the protective effects and related mechanisms of Qifuyin in AD mice to provide a theoretical reference for further exploration of the potential mechanism of Qifuyin in the treatment of AD.

Materials and Methods

Cell Lines, Animals and Reagents

Immune cells such as Raji cells, Jurkat cells, and RAW264.7 cells were generously gifted by Professor Ding Xiang from China West Normal University. All cell lines used in the experiments passed the biomedical ethics review of Yan'an University School of Medicine. Mice microglial BV2 cells were purchased from the Cell Bank of the Chinese Typical Culture Collection Center.

Twelve-week-old SPF-grade male APP/PS1 (Amyloid Precursor Protein/Presenilin 1) double-transgenic mice and seven weeks old SPF-grade female C57BL/6 mice were purchased from Nanjing Junke Bioengineering Co., LTD (animal license number: SCXK(Su)2021–0013). During the experiment, all mice were housed in Yan'an University Animal Experiment Center (the internal environment of the mice room was set as temperature: 24±2°C, relative humidity: 60% ±10%, day and night cycle: 12h/12h alternating light and dark), and the animals were provided with a standard diet,

Table 1 Primers for qPCR

Genes	Primer Sequences	
	Forward (5′–3′)	**Reverse (5′–3′)**
IL-6	GGGACTGATGCTGGTGACAA	CAACTCTTTTCTCATTTCCACGA
IL - 1β	CAGGCAGGCAGTATCACTCATT	CGTCACACACCAGCAGGTTATC
TNF-α	CCCAGACCCTCACACTCAGAT	AGCCTTGTCCCTTGAAGAGAA
AKT	CGCCTGCCCTTCTACAACCA	GGCCGTGAACTCCTCATCAA
RAGE	TGCTGGTTCTTGCTCTATGGG	TCCTTCACGAGTGTTTCTTTGC
NF-κB	TCCAAGACTACGACAGCCACAT	AGGAGCCTGATACTGGCACTTC
GAPDH	GAGTGTTTCCTCGTCCCGTAGA	CAACAATCTCCACTTTGCCACT

allowed to drink water and move freely. All animal experiments were performed in accordance with the Guide for the Care and Use of Laboratory Animals.

The chemicals, cell culture medium, antibodies, CCK-8 reagents, ELISA kits, and other materials used in the experiments were purchased from Beijing Solarbio Technology Co., Ltd. Amplification primers for qPCR were synthesized by Sangon Bioengineering Co., Ltd. (Shanghai) Co., LTD (Table 1). Zunyimycin C, Qifuyin, and Jiawei Qifuyin were prepared in our laboratory, according to their corresponding specifications.[7]

Targets Prediction of Jiawei Qifuyin on Alzheimer's Disease

The TCMSP and HERB databases were searched to screen various active ingredients in various TCM components of traditional Chinese medicine in Jiawei Qifuyin. Candidate active ingredients were imported into the TCMSP platform to query all potential targets of the candidate compounds, and the collected target names were standardized using the UniProt database to establish a component-target dataset. Anti-AD targets were collected from the Genecards database using "Alzheimer's disease" as the keyword, and the potential anti-AD targets of Jiawei Qifuyin were obtained by intersection with the targets of the active ingredients of Jiawei Qifuyin. The above targets were imported into VENNY2.1 for visual analysis.

The STRING database was used to construct a PPI map of protein interactions of intersecting genes, and Cytoscape 3.9.1 software was used to analyze the PPI network. The top 30 genes with degree values were selected as the key targets (the nodes were analyzed by color depth to reflect the degree value).

After the Metascape database was used to analyze the GO and KEGG pathways of intersection targets, the enrichment results were drawn into a bubble chart, and the potential biological functions and signaling pathways of Jiawei Qifuyin in the treatment of AD were obtained [18], following the top 10 enriched KEGG signaling pathways and pathway-related genes, to construct a relationship network using the Cytoscape software.

In vitro Antioxidant and Hydroxyl Radical Scavenging Capacity Assay

The Fe^{3+} reduction and Fenton reaction kits were used to determine the total antioxidant and hydroxyl radical scavenging capacities of the drugs in vitro, respectively.[8] Specific procedures were performed according to the manufacturer's instructions. That is to say, the final concentration of Jiawei Qifuyin was diluted to 1, 2, 4 and 8 mg/mL respectively to determine the total antioxidant capacity and hydroxyl radical scavenging capacity of the drug in vitro, and each sample was determined three times in parallel.

Effect of Drugs on the Proliferation of Immune Cells Assay

Jurkat, Raji, and RAW264.7, cells were cultured in RPMI-1640 medium to the logarithmic growth phase. The cells were digested with 0.25% trypsin, diluted with the same medium, diluted to a final density of 1×104 cells/mL, and then added at final concentrations of 1.25, 2.5, 5.0, 10.0 μg/mL, respectively. After culturing for 24h at 37°C in a 5% CO2 cell incubator, 10μL CCK-8 solution was added to each well, after 1.5 hours, the OD450 value was measured, and the corresponding cell survival rate was calculated. Four replicates were used for each group.

In vitro Anti-Neuritis Activity Assay

BV2 microglial cells were cultured in DMEM complete medium containing 10% FBS and 1% dual antibody (penicillin-streptomycin) until the logarithmic growth phase and diluted to a final density of 1×104 cells/mL. The cells were divided into a control group (without drug), 1μg/mL LPS treated group and 1μg/mL LPS plus 1.25, 2.5, 5.0, 10.0μg/mL Jiawei Qifuyin-treated groups, with four replicates per group. After being cultured in a cell incubator with 5%CO2 at 37°C for 7h, 10μL CCK-8 solution was added to each well, and the OD450 value was measured after 1.5h to evaluate the effect of modified Qifuyin on BV2 cell activity.

After cells were incubated, the medium in each well was collected and the supernatant was collected after centrifugation at 1000 rpm for 10min at 4°C. The inflammatory factors IL-2, IL-6, TNF-α, and IFN-γ were detected using ELISA, according to the manufacturer's instructions. The antineuritis activity of Jiawei Qifuyin was evaluated based on the effect of drugs on LPS-induced production of IL-6, IL-2, IFN-γ, and TNF-α by microglial BV2 cells.

In vivo Interventions for APP/PS1 Mice

All experimental mice (12 weeks old) were randomly divided into seven groups, and the detailed grouping information is shown in Table 2.

All the experimental mice were continuously treated with the corresponding drugs for 60 days. The administration of free drinking water was based on an average daily water consumption of approximately 8mL per mice, and the drug solution was prepared in combination with the dosage administered to each group of animals. According to the activity rules of the mice, they drank water normally during the day and changed to a water bottle containing the drug solution at 8 p.m. for free drinking.

The Morris water maze (MWM) was performed with reference to the previous literature after the drug intervention.[7] Morris water maze analysis system (Zhongshi DiChuang Technology Co., Ltd, Beijing, China) was used for this experiment. The MWM was performed in a circular pool (120 cm in diameter and 40 cm in height) filled with water (water height of 30 cm). The pool is divided into four quadrants. Mice in each group were placed into four quadrants of the water maze for four consecutive days, and the mice were trained at the same time every day. In each experiment, the time taken by the mice to find the escape platform was recorded as escape latency. Each mice was allowed to find the escape platform 60 times, and the mice that did not find the platform within 60s were manually guided to the platform by the tester and stayed on it for approximately 10s. After the 4 days positioning navigation experiment, mice were subjected to a space exploration experiment on 5day. The hidden escape platform was withdrawn and the mice were randomly placed in the water maze from a certain point and allowed to freely swam for 60s. The number of crossings of

Table 2 Grouping and Treatment of Mice

Name	Drug	Dosage mg/kg	Administration	Mice
NM	-	/	Free drinking	C57BL/6
BC	-	/	Free drinking	*APP/PS1*
PC	Donepezil	5.0	Free drinking	*APP/PS1*
LQ	Low-dose Qifuyin	20.0	Free drinking	*APP/PS1*
LMQ	Low dose Jiawei Qifuyin	20.0	Free drinking	*APP/PS1*
MMQ	Medium dose Jiawei Qifuyin	40.0	Free drinking	*APP/PS1*
HMQ	High dose Jiawei Qifuyin	80.0	Free drinking	*APP/PS1*
NaB	Sodium butyrate	12 00.0	Free drinking	*APP/PS1*
KZ	Zunyimycin C	3.2	Free drinking	*APP/PS1*
BZ	Zunyimycin C	5.2	Nose	*APP/PS1*
KL	Zunyimycin C+low dose Jiawei Qifuyin	3.2+20.0	Free drinking	*APP/PS1*
BL	Zunyimycin C+low dose Jiawei Qifuyin	5.2 + 20.0	Nose+Free drinking	*APP/PS1*

Notes: Zunyimycin C+low dose Jiawei Qifuyin: Zunyimycin C and low dose Jiawei Qifuyin are administered simultaneously; 3.2+20.0:Zunyimycin C was administered at a concentration of 3.2mg/kg, and low dose Jiawei Qifuyin was administered at a concentration of 20.0mg/kg; 5.2 + 20.0:Zunyimycin C was administered at a concentration of 5.2mg/kg, and low dose Jiawei Qifuyin was administered at a concentration of 20.0mg/kg; Nose+ Free drinking:Zunyimycin C was administered by nose, and low dose Jiawei Qifuyin was administered by free feeding and drinking.

the mice made through the original platform location was recorded. All behavioral parameters were tracked, recorded, and analyzed.

Immunofluorescence of Brain Tissue in APP/PS1 Mice

$A\beta_{1\text{-}42}$ in APP/PS1 expression in mice brain tissue Frozen sections were stored at room temperature, fixed with 4% paraformaldehyde (Shanghai Aladdin Biochemical Technology Co., Ltd). for 20 min at room temperature, and washed three times with 1×PBS for 5 min each. 1.5%H2O2, 15min, room temperature, 1×PBS three times, 5 min each time; 10% goat serum (Beijing Solarbio Science & Technology, China) 37°C for 30 min incubation; Discard the sealing fluid, add primary antibody working solution (Servicebio: GB111197-100, China), 4°C for the night; The primary antibody was rewarmed, washed three times with 1×PBS for 5 min each time, and the secondary antibody working solution was added (Boster Biological Technology: BA1135, China), incubated at room temperature for 1h, washed three times with 1×PBS for 5 min each time, and sealed with anti-fluorescence quenching tablet containing DAPI (Beijing Solarbio Science & Technology, China). The same visual field was selected for each group, and a fluorescent inverted microscope (Nikon, Japan) was used for observation at 20 × and 40 × magnified for 1–2 hours.

Analysis of Aβ Content in Mice Brain

Mice were anesthetized with an intraperitoneal injection of 1% sodium pentobarbital at a dose of 0.15mL/20g. No obvious response was observed with light tail pinching, indicating that the mice entered a state of deep anesthesia. The anesthetized mice were sacrificed by cardiac perfusion with normal saline. The skull was cut along the foramen magnum. The skull was opened using hemostatic forceps. When the olfactory bulb was exposed, the whole brain tissue was pulled from the anterior and inferior parts of the olfactory bulb using ophthalmic bend forceps and the cranial nerve at the skull base was cut off. The tissue was rinsed with precooled phosphate-buffered saline (PBS) to remove residual blood. For every 100 mg of tissue, 900μL of PBS solution was added and protease inhibitors were added to the tube to a final concentration of 1mM, which was mixed and ground using a tissue grinder. After grinding, the grinding solution was collected in a centrifuge tube, centrifuged at 1500rpm for 10min at 4°C, and the supernatant was collected for subsequent experiments. For specific experimental procedures, please refer to the instructions for the ELISA reagents.

Quantitative Real-Time PCR (qPCR)

After the behavioral experiment, the mice were anesthetized and perfused with normal saline and the brain tissue was removed, immediately placed in liquid nitrogen, 100 mg of mice brain tissue was added to 1mL of RNAiso Plus, and total RNA was extracted from the mice brain tissue using RNAiso reagent (TaKaRa, Osaka, Japan). The concentration and purity of the total RNA were determined using a microplate reader (MOLECULAR DEVICES, CA, USA). The PrimeScriptTMRT Master Mix (Perfect Real Time) kit (TaKaRa, Osaka, Japan) was used to reverse-transcribe RNA to cDNA. qPCR was performed using a Cobas z 480 (Roche Applied Science, Basel, Switzerland). cDNA was analyzed using the TB Green Premix Ex TaqTM (Tli RNaseH Plus) kit (TaKaRa, Osaka, Japan). GAPDH served as an endogenous control. The primers used for qRT-PCR are listed in Table 1. The obtained Ct value and the ΔCt, ΔΔCt, and 2-ΔΔCt values of each gene were calculated to analyze the changes in mRNA expression levels.

Intestinal Flora Assay

One day before the end of the drug intervention, the mice were induced to defecate by tail lifting, and feces were collected and placed in a sterile Eppendorf tube with sterilized forceps. The samples were stored in at −80°C refrigerator immediately after collection. The intestinal microbiota of the mice was determined using 16SrDNA amplicon sequencing. The experiment was conducted by Shanghai Zhongke New Life Biotechnology Co., Ltd. The specific experimental process was as follows: whole-genome DNA was extracted using the CTAB/SDS method, and DNA concentration and purity were monitored on 1% agarose gel.

16SV3-V4:341F-806R, 18SV9:1380F-1510R, ITS1: ITS1F-ITS2R primers for 16S/18S rRNA gene amplification using specific primers with barcodes. All PCR reactions were performed in a 30μL reaction with 15 μL Phusion® high-fidelity PCR premix, and PCR amplification products were identified by electrophoresis on 2% agarose gels. The PCR

products of the mixture were purified using the AxyPrep DNA Gel Extraction Kit (AXYGEN) and prepared using the NEB NextUltraDNA Library Kit. Library quality was assessed using a fluorimeter (Qubit@2.0) and Agilent Bioanalyzer 2100 system. Finally, the libraries were sequenced on an Illumina Miseq/HiSeq2500 platform and 250bp/300bp paired end read sequence information was generated. The paired-end reads from the original DNA fragments were merged using the FLASH software. Paired-end reads were assigned to each sample using a unique barcode.

Sequence analysis was performed using the UPARSE software package with the UPARSE-OTU and UPARse-other algorithms. Sequences with ≥97% similarity were assigned to the same OTU. The OTU table was then rarefied and three metrics were calculated: Chao1 estimated species abundance, the number of unique otus in each sample was estimated by observed species, and the Shannon index was calculated. Rarity curves are generated based on these three metrics.

SCFA Assay

Fecal short-chain fatty acids (SCFAs) were obtained from Shanghai Zhongke New Life Biotechnology Co., Ltd. Nine hundred microliters of 0.5% phosphate solution was used to resuspend 30 mg of the fecal samples. After centrifugation at 12000 rpm for 10 min, the supernatant was collected, added to an equal volume (approximately 800 μL), and extracted by shaking for 20 min in ethyl acetate. Then, centrifuge at 12000 rpm for 10 min, and 600 μL of the upper organic phase was mixed with 4-methylvalaric acid (final concentration 500μM) as an internal standard and then added into the injection bottle for GC-MS detection. MSD ChemStation software was used to extract the chromatographic peak areas and retention times. A standard curve was drawn to calculate the SCFA content of the samples.

Statistical Analysis

Statistical analysis and mapping of the data were performed using GraphPad Prism 8 software and are presented as mean ± standard deviation (mean±SD). One-way ANOVA was used to analyze the difference in data between multiple groups, and statistical significance was set at $P<0.05$.

Results

Pathway Involved in the Treatment of AD with Jiawei Qifuyin

According to the screening conditions of the active ingredients and action targets, 46 active ingredients and 521 targets of Jiawei Qifuyin were identified. The intersection genes of Jiawei Qifuyin and AD were obtained and 105 targets were found to be related to AD. The top 30 targets were imported into Cytoscape 3.9.1 software to draw a PPI network diagram. AKT1, TNF, JUN, IL1ß, and PTGS2 were the five most important nodes with high degree values, indicating that these proteins may have important significance in the PPI network and may be key targets of Jiawei Qifuyin against AD. The biological process (BP), cellular component (CC), and molecular function (MF) of the intersection targets were analyzed using Metascape, and the results indicated that BP was mainly manifested in the response of cells to organic cyclic compounds, hormones, lipopolysaccharides, and synaptic signal transduction. The main manifestations were membrane rafts, postsynaptic membranes, dendrites and receptor complexes. For CC, neurotransmitter receptors, nuclear receptors, oxidoreductase activity, and kinase binding are the main activities. KEGG pathway enrichment analysis was performed on the intersecting genes, and the top 20 signaling pathways were selected for visual analysis. The results indicated that the targets were mainly enriched in lipids and atherosclerosis, neuroactive ligand-receptor interaction, the AGE-RAGE signaling pathway in diabetic complications, and the PI3K-Akt signaling pathway.[9–11] Most of these pathways are related to inflammation, suggesting that Qifuyin may interfere with AD by inhibiting the inflammatory signaling pathway.

The obtained KEGG pathways were imported into Cytoscape 3.9.1 software, and the top 10 significantly enriched KEGG pathways and pathway-related genes were intersected to obtain Figure 1. It can be seen that hsa05022, hsa05417, and hsa04080 were the signaling pathways with a large number of enriched genes, and AKT1 and PTGS2 were the genes with a large number of enriched genes and were involved in more pathways. Network pharmacology results suggest that AKT is the core gene of Jiawei Qifuyin in the treatment of AD and that the AGE/RAGE signaling pathway is one of the

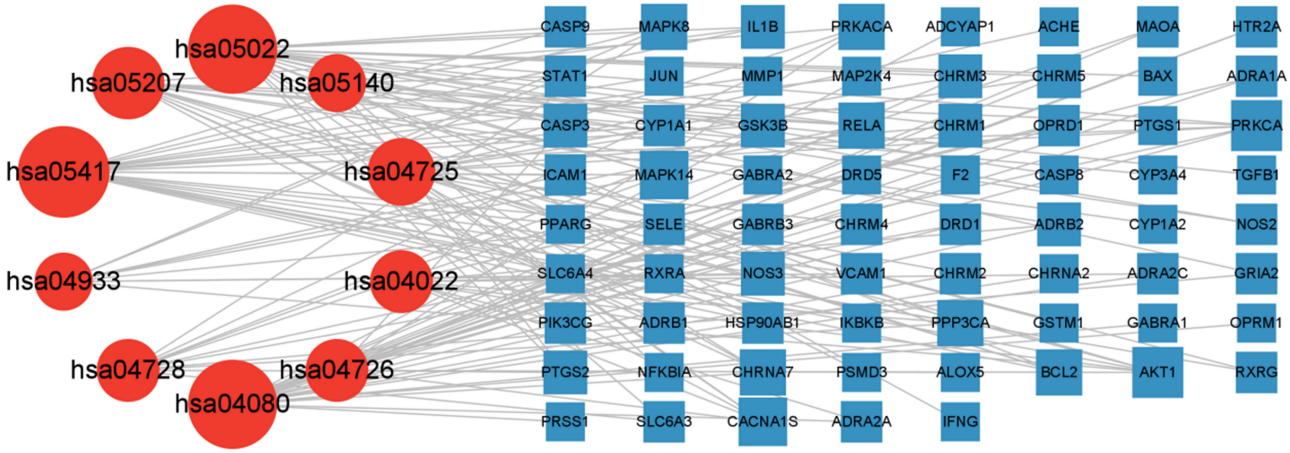

Figure 1 Predicted pathway and gene network in the treatment of AD with Jiawei Qifuyin. Red Circle: the KEGG signaling pathway. Blue bar: the protein related to the pathway. The area of the two nodes is related to the degree value, and the higher the degree value, the larger the area.

key pathways of Jiawei Qifuyin in the treatment of AD. Therefore, the mechanism of Jiawei Qifuyin in the treatment of AD can be further explored based on the AGE/RAGE/AKT pathway.[12]

In vitro Antioxidant and Hydroxyl Radical Scavenging Capacity of Jiawei Qifuyin

Based on the results of the preliminary experiment, gradient concentrations of 1.0, 2.0, 4.0, and 8.0 mg/mL were used for the in vitro antioxidant test of Jiawei Qifuyin. The results showed that the total antioxidant capacity of Jiawei Qifuyin in vitro was concentration-dependent within the measured concentration range (Figure 2A). The hydroxyl free radical scavenging ability of 8.0 mg/mL Jiawei Qifuyin was significantly higher than that of 1.0, 2.0, and 4.0 mg/mL modified Qifuyin (Figure 2B).

Effect on the Proliferation of Immune Cells of Jiawei Qifuyin

Effects of different concentrations of Jiawei Qifuyin on the proliferation of Jurkat cells, Raji cells, and RAW264.7 cells were analyzed and the results showed that after 24 hours of treatment with different concentrations of Jiawei Qifuyin, compared with the control group, 5.0μg/mL Jiawei Qifuyin could promote the proliferation of Jurkat cells (Figure 3A), however, Raji cells were more sensitive to the drug and showed the effect of promoting cell proliferation within the concentration range selected in the experiment (Figure 3B), while 10.0μg/mL Jiawei Qifuyin could significantly promote the proliferation of RAW264.7 cells (Figure 3C).

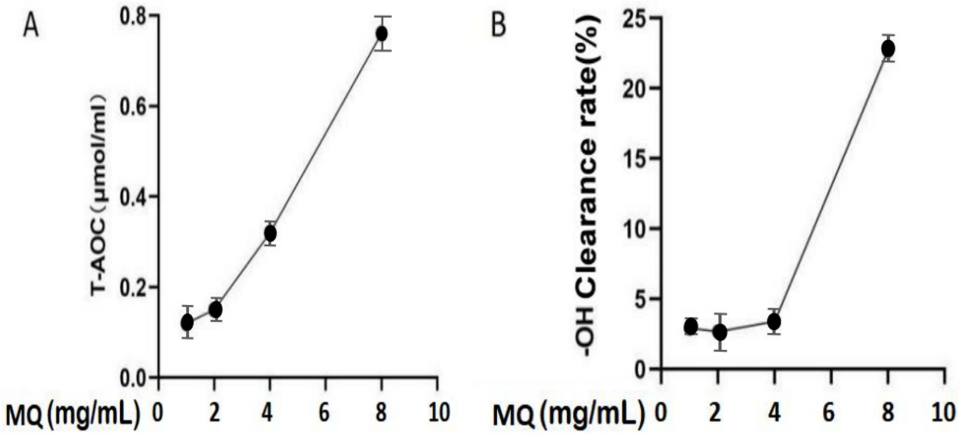

Figure 2 (**A**) Antioxidant capacity of Jiawei Qifuyin. (**B**) Hydroxyl radical scavenging capacity of Jiawei Qifuyin.

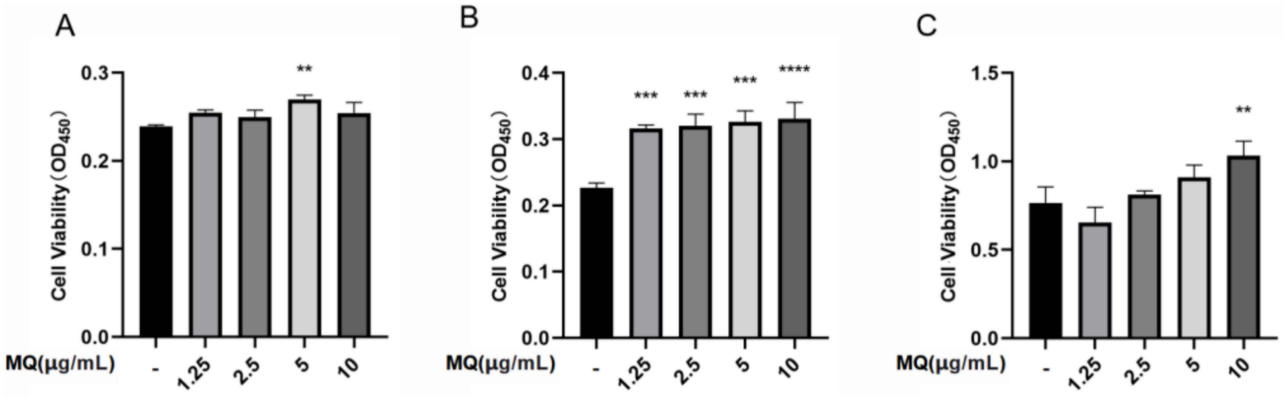

Figure 3 Effects of Jiawei Qifuyin on immune cell proliferation. (**A**) Jurkat cells. (**B**) Raji cells. (**C**) RAW264.7 cells. ***P* < 0.01, ****P* < 0.001, *****P* < 0.0001.

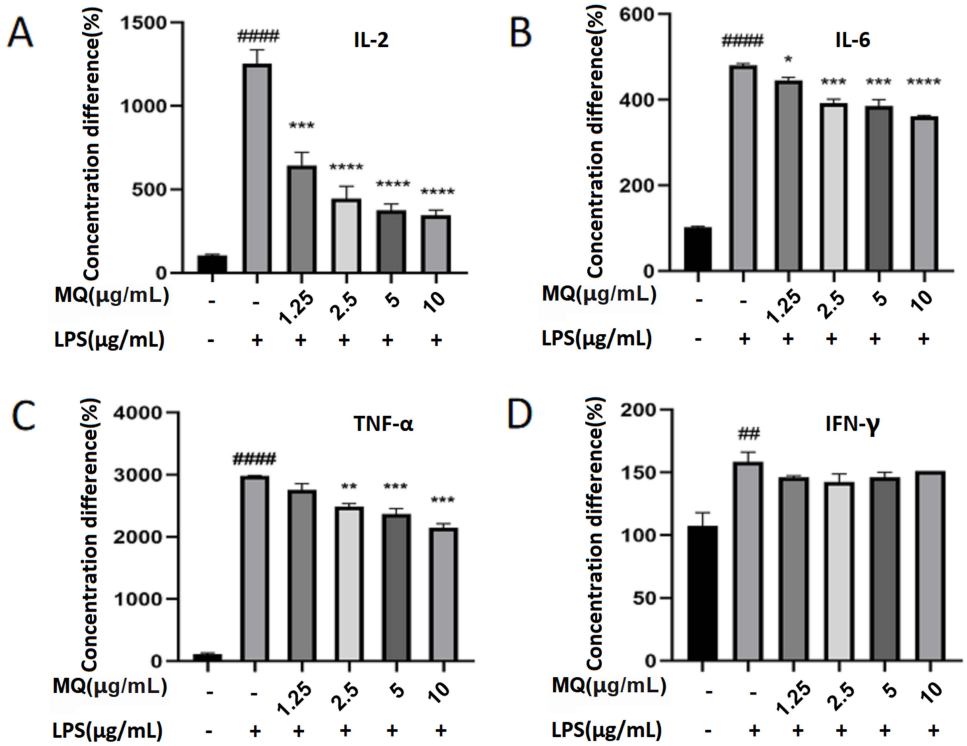

Figure 4 Effect of Jiawei Qifuyin on inflammatory factors from LPS-activated BV-2 cells. (**A**) IL-2. (**B**) IL-6. (**C**) TNF-α. (**D**) IFN-γ. ##*P*< 0.01; ####*P*< 0.0001 vs blank group; **P* < 0.05, ***P* < 0.01, ****P* < 0.001, *****P* < 0.0001.

In vitro Anti-Neuritis Activity of Jiawei Qifuyin

ELISA was used to detect the effects of different concentrations of Qifuyin on the LPS-induced release of related inflammatory factors in BV2 cells, and the results showed that compared with the control group, the release of the four inflammatory factors was significantly increased after LPS induction, indicating that LPS promoted the activation of BV2 cells. Compared to the LPS-induced BV2 cell model group, 1.25, 2.5, 5.0, and 10.0μg/mL Jiawei Qifuyin inhibited the release of IL-2, IL-6, and TNF-α in a dose-dependent manner (Figure 4A–C), whereas there was no significant change in the release of IFN-γ (Figure 4D). These results indicate that Qifuyin significantly inhibited the secretion of pro-inflammatory cytokines, such as IL-2, IL-6, and TNF-α, in LPS-stimulated BV-2 cells within a certain concentration range.

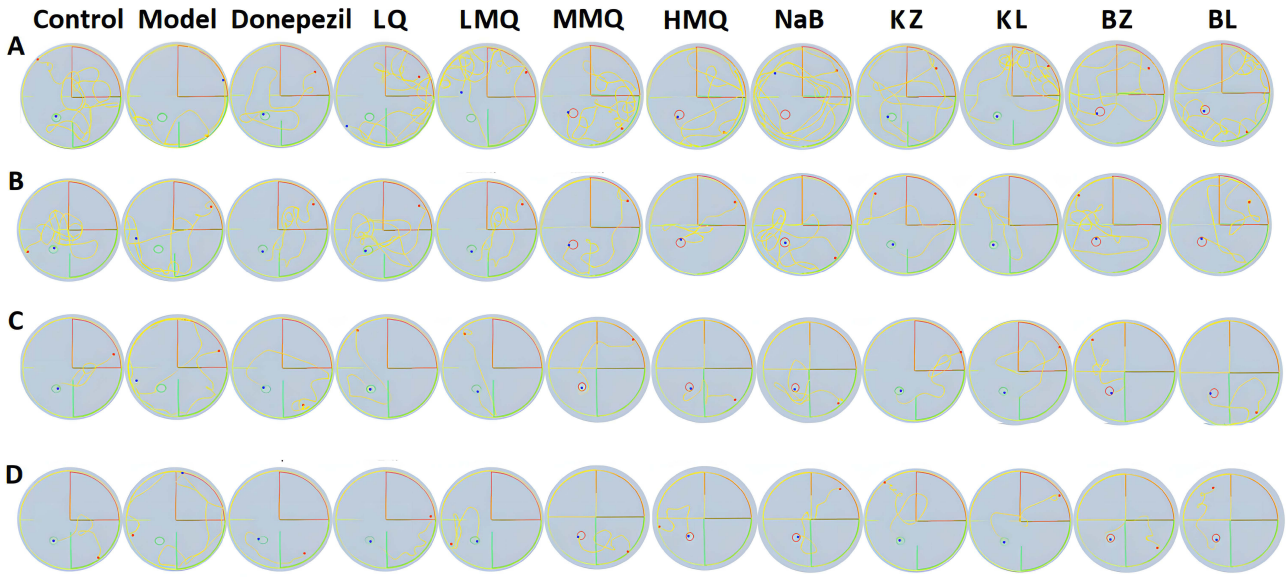

Figure 5 Four-day positioning navigation experiment trajectory map of mice. (**A**) 1st day. (**B**) 2nd day. (**C**) 3rd day. (**D**) 4th day. Red point: starting point of swimming. Blue points: end point of swimming.

Effects of Drugs on Learning and Memory Impairment in APP/PS1 Mice

To evaluate the effects of the different drug interventions on the cognitive function of mice in each group, the Morris water maze test was used to assess the spatial memory ability of mice in each group. The localization navigation experiment of each group of mice after consecutive 4-day training were detected (Figure 5) while the escape latency of each group of mice after 4-day continuous training were counted and the results (Figure 6) shows that from the first day

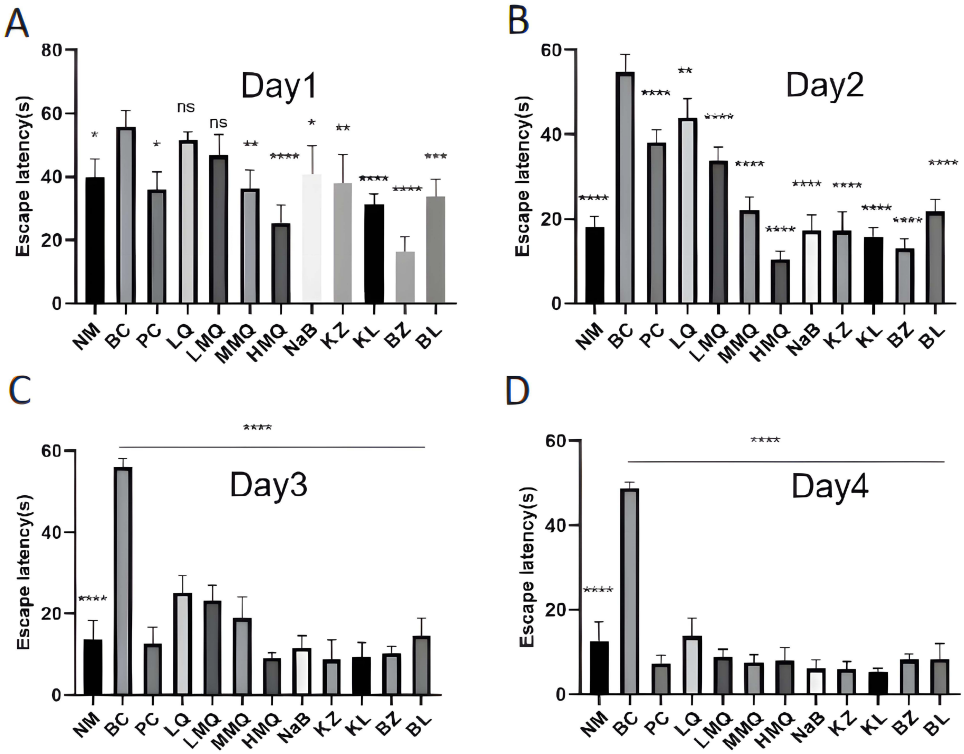

Figure 6 Effects of drugs on the latency period of APP/PS1 mice. (**A**) Day1. (**B**) Day2. (**C**) Day3. (**D**) Day4. n=6; **P* < 0.05, ***P* < 0.01, ****P* < 0.001 and *****P* < 0.0001.

of training, the escape latency of the APP/PS1 blank control group (BC) was significantly higher than that of the normal group (NM), and the results were statistically significant ($P < 0.05$). The escape latency of the PC and positive control groups was significantly lower than that of the BC group from the first day ($P < 0.05$). From the second day, the escape latency of each group of mice was significantly lower than that of the BC group, and the results were statistically significant ($P < 0.01$). At the same time, it can be seen from the results that the escape latency of each drug intervention group on the 3rd and 4th day was statistically significant compared to that of the BC group ($P < 0.0001$), and gradually approached that of the NM group, even lower than that of the NM group, indicating that the above drugs can improve the learning and memory ability of APP/PS1 transgenic mice.

The statistical results of the number of times each group of mice crossed the platform after a 4-day positioning navigation experiment were shown (Figure 7A) that the number of times the NM group mice crossed the platform was

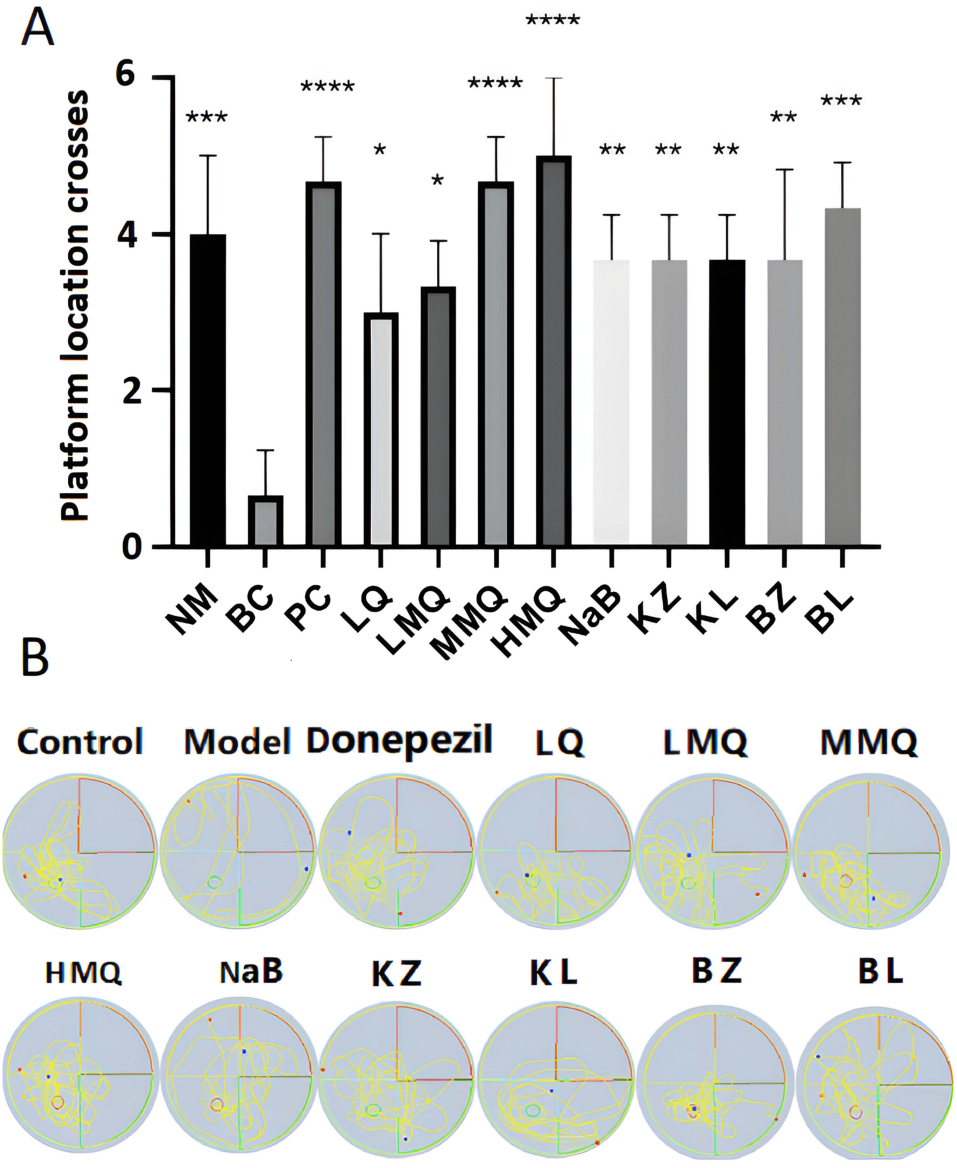

Figure 7 (**A**) Effects of drugs on the number of plateau crossings in APP/PS1 mice. (**B**) Experimental trajectory plot of mouse space exploration in different drug intervention groups. n=6; *$P < 0.05$, **$P < 0.01$, ***$P < 0.001$ and ****$P < 0.0001$.

Note: Model:APP/PS1 blank control group.

Abbreviations: NM, normal control group; Donepezil, donepezil positive group; LQ, low dose Qifuyin; LMQ, low-dose modified Qifu yin; MMQ, medium dose modified Qifu yin; HMQ, high-dose modified Qifu yin; NaB, butyrate intervention group; KZ, zunyimycins orally; KL, zunyimycins and low dose Qifu yin; BZ, transnasal zunyimycins; BL, transnasal zunyimycins and oral low-dose modified Qifu yin.

significantly higher than the BC group, with a statistical difference (P<0.001). The platform crossing times of the LQ and LMQ intervention groups were 3.33±0.94 and 3.33±0.47, respectively, which were higher than that of the BC group (0.67 ±0.47), and the results were statistically significant (P<0.05). The number of platform crossings in the NaB, oral Zunyimycin C(KZ), oral Zunyimycin C, low-dose Jiawei Qifuyin (KL), and transnasal Zunyimycin C (BZ) intervention groups was higher than that in the BC group, and the results were statistically significant (P<0.01). The number of times the remaining drug intervention group mice crossed the platform was higher than that of the BC group, and also higher than that of the NM group (P<0.0001), indicating that these APP/PS1 transgenic mice recovered their spatial memory ability well after drug intervention.

The trajectory analysis of each group of mice in the spatial exploration experiment is shown (Figure 7B), except for the APP/PS1 blank control group (Model) mice, which moved randomly in the pool; the experimental trajectory was irregular, and the number of crossings was lower. Mice in the other drug intervention groups moved more frequently at the original platform location and crossed the platform more frequently.

Effects of Drugs on Aβ Content in the Brain of APP/PS1 Mice

Immunofluorescence staining of amyloid plaques was performed to investigate whether zunyimycins and Jiawei Qifuyin had beneficial effects on Aβ aggregation in APP/PS1 mice. We observed that LQ, LMQ, and KL significantly reduced Aβ aggregation in the brains of APP/PS1 mice (Figure 8), which is consistent with the results of the APP/PS1 control group compared with LQ, LMQ, and KL, which reduced the cerebral cortex and hippocampal Aβ levels (Figure 8), indicating that zunyimycins treatment with Qifuyin alleviated Aβ aggregation in APP/PS1 mice.

After different drug interventions, A levels in the brain tissue of mice in each group $A\beta_{1\text{-}40}$ and $A\beta_{1\text{-}42}$ the results of changes in content are shown (Figure 9); the content of $A\beta_{1\text{-}40}$ in the brain tissue of APP/PS1 transgenic mice in the BC group was significantly higher than that of normal mice in the NM group, and the results were statistically significant (P<0.0001). In addition, different drug interventions significantly reduced the $A\beta_{1\text{-}40}$ content in the brain tissue of APP/PS1 transgenic AD mice, and the results were statistically different (P<0.0001), indicating that the drugs used in this experiment could improve the clearance ability of $A\beta_{1\text{-}40}$ in the brain tissue of APP/PS1 mice to a certain extent; however, the specific mechanism is not clear (Figure 9A).

The changes of $A\beta_{1\text{-}42}$ content in the brain tissue of each group of mice after different drug interventions shown (Figure 9B) that the $A\beta_{1\text{-}42}$ content in the brain of APP/PS1 transgenic mice in the BC group was significantly higher than that of normal mice in the NM group, and the results were statistically significant (P < 0.01). Compared to the BC group, the $A\beta_{1\text{-}42}$ content in the LQ, LMQ, MMQ, HMQ, NaB, and BZ groups decreased significantly (P< 0.01), whereas the other groups showed no significant changes. These results indicated that the above drugs promoted the clearance of $A\beta_{1\text{-}42}$ in the brain tissue. In addition, we found that the LMQ and NaB intervention groups had lower levels

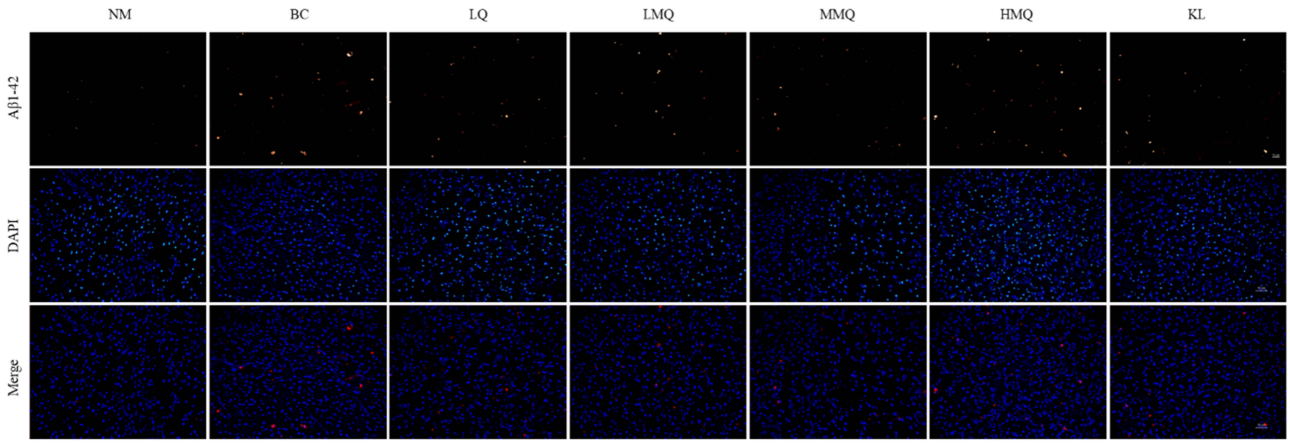

Figure 8 Immunofluorescence of brain tissue in APP/PS1 mice, scale bar, 25 μm.
Notes: Zunyimycins and Jiawei Qifu decoction reduced Aβ accumulation in APP/PS1 mice. Immunofluorescence was used to detect the content of small mice inside Aβ.

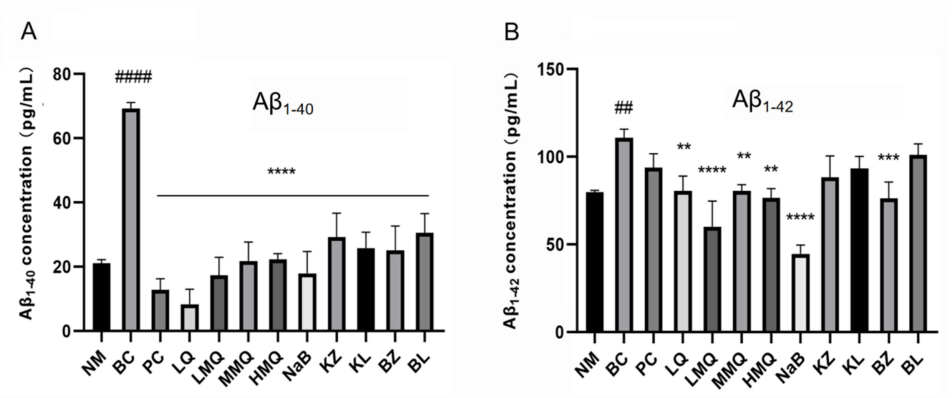

Figure 9 (**A**) Effects of different drug on Aβ $_{1-40}$content in the brain of APP/PS1 mice. (**B**) Effects of different drug on Aβ $_{1-42}$content in the brain of APP/PS1 mice. n=4. $^{\#\#}P$< 0.01. $^{\#\#\#\#}P$<0.0001.$^{**}P$ < 0.01, $^{***}P$ < 0.001 and $^{****}P$ < 0.0001.

of $A\beta_{1\text{-}42}$ in the brain tissue of APP/PS1 mice, indicating that low doses of Jiawei Qifuyin and sodium butyrate had a stronger clearance ability of $A\beta_{1\text{-}42}$ in the brain tissue of APP/PS1 mice.

Effects of Drugs on mRNA Expression of Neuroinflammatory Factors in APP/PS1 Mice

The differential expression changes of mRNA of some inflammation-related and pathway-related genes in the brain tissue of each group after drug intervention compared with the blank group are shown in Figure 10 and the results showed that compared with the BC group, the donepezil intervention group upregulated the expression of IL-6 and downregulated the expression of RAGE and NF-κB. Low-dose Qifuyin upregulated the expression of TNF-α and AKT and downregulated the expression of IL-6, IL-1β, RAGE, and NF-κB. Low-dose Qifuyin upregulated the expression of NF-κB and downregulated the expression of IL-1β, IL-6, and RAGE. Medium-dose Qifuyin upregulated the mRNA expression of AKT and NF and downregulated the mRNA expression of TNF-α and IL-1β. High-dose Qifuyin upregulated the mRNA expression of AKT, RAGE, and NF- and downregulated the mRNA expression of IL-1β. The butyrate intervention group showed increased mRNA expression of TNF-α, AKT, and NF-κB and decreased mRNA expression of IL-1β, IL-6, and RAGE. The oral Zunyimycin C intervention group showed downregulated RAGE mRNA expression and upregulated AKT and NF-κB mRNA expression. The oral Zunyimycin C combination group down-regulates the expression of IL-1β and upregulates RAGE, AKT, and NF-κB expression. The transnasal Zunyimycin C intervention group showed downregulated RAGE and IL-6 expression and upregulated NF-κB expression. The expression of IL-6 and NF-κB was downregulated in the transnasal Zunyimycin C combination group.

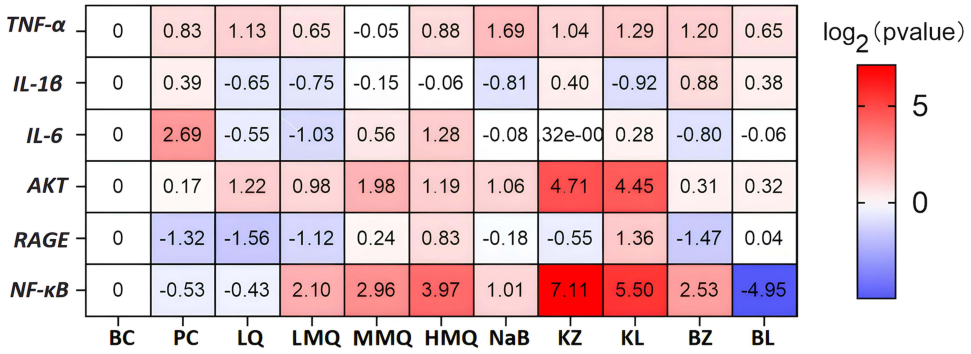

Figure 10 mRNA expression of inflammatory factor in brain tissues in APP/PS1 mice. n=6.

Effects of Pharmacologic Interventions on the Intestinal Flora in APP/PS1 Mice

Cluster analysis of the OTUs of the intestinal flora of mice from different experimental groups showed a total of 244 identical OTUs among all the experimental groups, whereas the unmedicated C57 mice (NM, 836 OTUs) had the highest number of unique OTUs when compared to the APP/PS1 with no pharmacological interventions (BC, 735 OTUs), and among the pharmacologically-treated mice, the low-dose Jiawei Qifuyin (LMQ, 769 OTUs), the butyrate intervention (NaB, 736 OTUs), and the medium-dose Jiawei Qifuyin (MMQ, 787 OTUs) had a slight increase in the number of specific OTUs, and the low-dose Qifuyin had just the same number of specific OTUs. In contrast, the number of specific OTUs was the lowest in the high-dose Jiawei Qifuyin (HMQ, 636 OTUs). For zone C, the number of specific OTUs was increased in both the oral drinking water combined with low-dose Jiawei Qifuyin (KL, 799 OTUs), transnasal drug delivery (BZ, 689), and drinking water administration groups (KZ, 692 OTUs), and the number of unique OTUs decreased. Low-dose Qifuyin showed the same number of unique 735 OTUs as those in BC (Figure 11).

Hierarchical cluster analysis of the diversity and abundance of enterobacteria among samples based on community composition at the phylum level yielded a Weighted Unifrac evolutionary tree calculated based on evolutionary information among microbial sequences and abundance information of OTUs.

The similarity between different samples can be investigated by performing cluster analysis of the samples, which showed (Figure 12A) that they clustered into two major clusters, in which the LQ, LMQ, and MMQ groups clustered together, and these three TCM-treated groups clustered into one major cluster, as did the group with the oral antibiotic zunyimyicn C, and the normal C57 mice as well as the AD mice intervened with the use of Donepezil, etc., while, surprisingly, HMQ clustered into another major cluster, as did the NabB, KZ, BZ, BC, and BL groups. Surprisingly, HMQ clustered into another large cluster with the NabB, KZ, BZ, BC, and BL groups. By analyzing the community structure of each sample or subgroup at different taxonomic levels, it was possible to visualize the species and their proportions with higher relative abundances at different taxonomic levels. Based on the results of the species annotation, the top 10 species in terms of maximum abundance at each taxonomic level, including Phylum, Class, Order, Family, Genus, Species, were selected for each subgroup to generate a bar chart of the relative abundance of species. Bacteroidetes, Firmicutes, Proteobacteria, Verrucomicrobia, Epsilon bacteraeota, Actinobacteria, Patescibacteria, and Tenericutes in the following order: Deferribacteres, Cyanobacteria, and others. Among them, the LQ, LMQ, and MMQ groups all showed a lower abundance of Bacteroidetes than Firmicutes, whereas Epsilonbacteraeota had a higher abundance than all other groups. Surprisingly, the abundance of Verrucomicrobia increased significantly in the HMQ

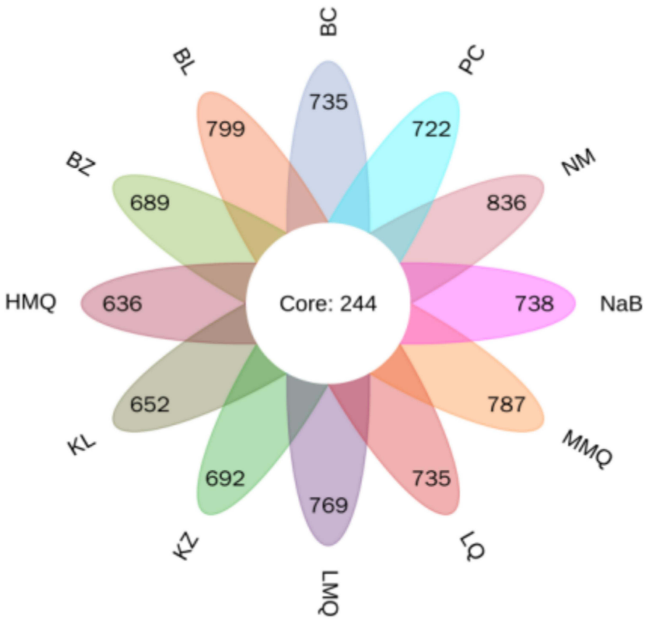

Figure 11 Petal plot based on OTUs distribution.

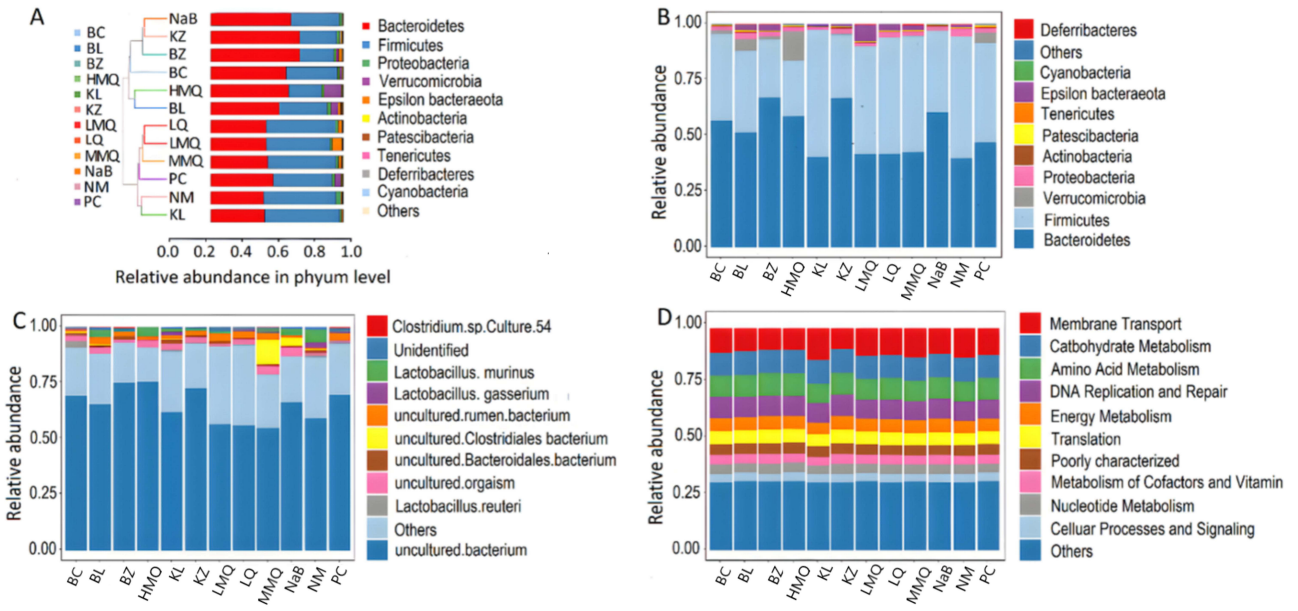

Figure 12 Effect of drugs on intestinal flora community in APP/PS1 mice. (**A**) UPGMA clustering tree and community structure. (**B**) Relative abundance at Phylum level. (**C**) Relative abundance at species level. (**D**) Relative functional abundance of KEGG.

group while at the same time the abundance of Firmicutes decreased significantly (Figure 12B). Similarly, the results of the community structure analysis at the species level (Figure 12C) showed that the known species with higher abundance were mainly Lactobacillus reuteri, Lactobacillus murinus, Lactobacillus gasserium, and Clostridium sp. Culture.54, the remaining strains were non-culture-identified and occupied the maximum abundance. In the MMQ group, non-cultured Clostridiales bacterium and rumen bacterium were significantly more abundant. Furthermore, by analyzing the functional composition and relative abundance of the bacterial groups in each subgroup, we found that (Figure 12D). The TOP ten KEGGs in the middle LQ, LMQ, and MMQ groups showed similar functional clustering.

Effects of Drugs on Intestinal SCFAs Metabolism in AD Mice

MSD ChemStation software was used to extract the chromatographic peak area and retention time according to the signal information of mass spectrometry of different concentrations of the standard substance. As shown in the figure, the content of seven SCFAs in the BC group was lower than that in the NM group, indicating that the content of SCFAs in the feces of APP/PS1 transgenic mice was different from that in normal C57 mice. In addition, the SCFA content in the feces of APP/PS1 transgenic mice was different from that in normal C57 mice after drug intervention.

The content of caproic acid and isovaleric acid in the PC group did not reach the same level as that in the NM group, and the content of the other five SCFAs exceeded that of the NM group, indicating that donepezil can reverse the level of intestinal metabolites in APP/PS1 transgenic mice to a certain extent. Compared with the BC group, we found that the content of seven types of SCFAs in the intestines of HMQ group mice was significantly increased and exceeded that of NM group mice, indicating that high-dose Jiawei Qifuyin can help restore the metabolite content in the intestines of APP/PS1 transgenic mice.

Changes in SCFAs in the intestines of APP/PS1 transgenic mice were also different between the KZ and BZ groups. Only valeric and isovaleric acids were recovered in the KZ group, whereas the contents of six SCFAs in the BZ group were higher than those in the BC group, except for caproic acid. These results indicate that different Zunyimycin C administration methods have different effects on the intestinal metabolites in APP/PS1 transgenic mice. Except for acetic acid and isovaleric acid, the other five short-chain fatty acids in the NaB group were higher than those in the BC group, indicating that butyrate can also promote the recovery of intestinal metabolites in APP/PS1 mice to a certain extent. The effects of different drug interventions on the intestinal short-chain fatty acid content of APP/PS1 mice were analyzed (Figure 13). Figure 13A showed that compared with the BC group, the acetic acid content of MMQ, NaB, KZ,

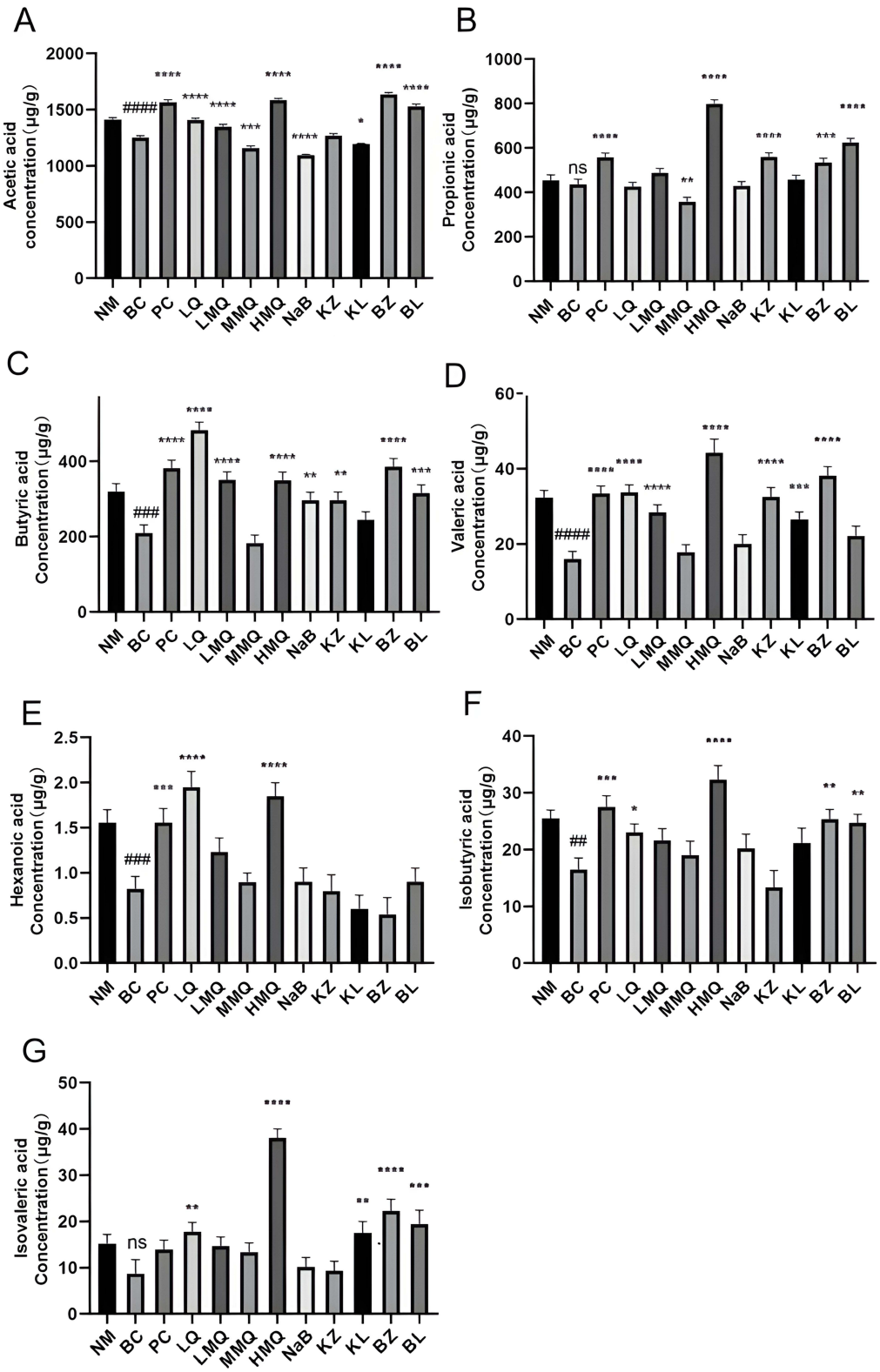

Figure 13 Effects of different drug interventions on intestinal short-chain fatty acid content in mice. (**A**) acetic acid content; (**B**) propionic acid content; (**C**) butyric acid content; (**D**) valeric acid content; (**E**) caproic acid content; (**F**) isobutyric acid content; (**G**) isovaleric acid content; $^{\#\#}P < 0.01$, $^{\#\#\#}P < 0.001$, and $^{\#\#\#\#\#}P < 0.0001$ vs NM group; n=4; $^{*}P < 0.05$, $^{**}P < 0.01$, $^{**}P < 0.001$, and $^{****}P < 0.0001$ vs BC group.

Abbreviation: ns, not statistically significant.

and KL groups decreased, and the acetic acid content of PC, LQ, LMQ, HMQ, BZ, and BL groups increased, and the results were significantly different ($P < 0.05$). Figure 13B shows that compared with the BC group, propionic acid content in PC, HMQ, KZ, BZ, and BL groups increased ($P < 0.01$). These results indicated that donepezil, high-dose Jiawei Qifuyin, oral Zunyimycin C, transnasal Zunyimycin C, and transnasal Zunyimycin C + oral low-dose Jiawei Qifuyin could improve the production of propionic acid in the intestine of APP/PS1 transgenic mice. Figure 13C shows that compared with the BC group, except for the medium-dose Jiawei Qifuyin (MMQ) group and the oral Zunyimycin C + low-dose Qifuyin (KL) group, the other drugs promoted the production of propionic acid in the intestines of the APP/PS1 mice ($P < 0.01$). Figure 13D shows that compared with the BC group, the ability of the PC, LQ, LMQ, HMQ, KZ, KL, and BZ groups to produce valeric acid increased ($P < 0.001$), and there was no significant change in the other groups. Figure 13E showed the changes in caproic acid content, and the results showed that compared with the BC group, the PC, LQ, and HMQ groups had an increase in caproic acid content ($P<0.001$), while the other groups have no significant changes. Figure 13F showed the changes of isobutyric acid content in the isobutyric acid content in PC, LQ, HMQ, BZ, and BL groups was significantly higher than that in the BC group ($P < 0.05$). Figure 13G shows the changes in isovaleric acid content. The isobutyric acid content of the LQ, HMQ, KL, BZ, and BL groups was higher than that of the BC group ($P < 0.01$), whereas the other groups showed no significant changes. These results indicate that different drugs have different effects on intestinal metabolites in APP/PS1 mice, which may be related to changes in the abundance of intestinal flora.

Discussion

In recent years, the relationship between the intestinal microbiota and human health has received increasing attention. Changes in intestinal microbiota can affect the host immune system, leading to disease states in the body. Research has found that Significant changes in the intestinal bacterial composition can be observed in patients with inflammatory bowel disease, allergies, autoimmune diseases, and some lifestyle-related diseases. Therefore, studying changes in the composition, structure, function, and metabolites of the intestinal flora can reveal their relationship with the occurrence and development of AD, which has practical significance for proposing new treatment methods and preventive measures in the future. Increasing evidence has shown that there is a bidirectional channel system between the gastrointestinal tract and brain, and the intestinal microbiota plays a crucial role in this communication. Therefore, the concept of intestinal microbiota and the brain axis, also known as the gut-brain axis, has emerged. With the proposal of the concept of the gut-brain axis, some studies have found that disorders of the gut-brain axis may be one of the pathogeneses of neurodegenerative diseases, such as AD. Studies have shown that changes in the composition of intestinal microbiota induce increased intestinal barrier permeability and immune activation, leading to systemic inflammation, which in turn may lead to neuroinflammation and neurodegeneration in the central nervous system. In addition, an increasing number of experimental and clinical studies have confirmed that the intestinal microbiota can regulate the host's cognitive function by promoting the host's metabolism to produce short-chain fatty acids. Therefore, this study mainly investigated changes in the intestinal microbiota and its metabolites in AD mice after intervention with Jiawei Qifuyin. This study further explored the role of the gut-brain axis, intestinal microbiota, and their metabolites in the pathogenesis of AD, providing a new therapeutic target for AD.

In this study, we investigated the effects of different drug interventions on the structural distribution, function, and short-chain fatty acids of the intestinal microbiota in APP/PS1 transgenic AD mice. The results of OTU values, gut microbiota diversity index, and microbiota abundance index between groups indicated that different drugs had different effects on the OTUs of mice microbiota. The combination of low and medium doses of Jiawei Qifuyin (LMQ, MMQ), sodium butyrate (NaB), and transnasal Zunyimycin C combined with oral low-dose Jiawei Qifuyin (BL) resulted in an increase in the number of unique OTUs in the intestinal tract of mice after the intervention, indicating that the intervention of the above drugs can improve the diversity of the APP/PS1 transgenic mice microbiota. However, the mechanism by which they improve the diversity of the microbiota remains unclear. Studies have found that an increase in the abundance of Bacteroidetes can promote the fermentation of polysaccharides and other substances to produce short-chain fatty acids, thereby affecting the host nervous system and delaying neuroinflammation. Proteobacteria is closely associated with inflammation. As a low-abundance bacterium in the gut of healthy individuals, its increase in abundance

is generally considered a potential diagnostic criterion for dysbiosis and disease risk. According to the changes in the abundance of intestinal flora in each group after drug intervention, compared with the APP/PS1 blank group, the high-dose Jiawei Qifuyin (HMQ), sodium butyrate (NaB), oral Zunyimycin C (KZ) and transnasal Zunyimycin C (BZ) intervention groups had an increase in the abundance of Bacteroidetes. The intervention group treated with low-dose Jiawei Qifuyin (LMQ) and oral zunymycins combined with Jiawei Qifuyin (KL) showed a decrease in the abundance of Proteobacteria, indicating that these drugs may inhibit the inflammatory response of the nervous system by increasing the abundance of Bacteroides and reducing the abundance of Proteobacteria, thereby delaying AD progression. In addition, KEGG and COG functional prediction results showed that changes in intestinal flora after intervention with different drugs may affect membrane transport, signal transduction mechanisms, transcription, carbohydrate transport, and metabolism, suggesting that these drugs may improve the intestinal microecological environment by affecting the function of intestinal flora and thus play a protective role in AD.

As an important "metabolic organ" in the human body, the intestinal microbiota is closely related to many physiological functions such as immunity, nutrition, and metabolism. Intestinal microorganisms can produce SCFAs by fermenting structural carbohydrate oligosaccharides, nonstarchy polysaccharides, and resistant starch. SCFAs, also known as volatile fatty acids, include acetic, propionic, butyric, isobutyric, valeric, isovaleric, caproic, and isocaproic acids. SCFAs play important roles in the regulation of cell proliferation and differentiation, apoptosis, immune response, energy metabolism, nutrient absorption, and lipid metabolism. In recent years, SCFAs produced by intestinal metabolism have been found to affect AD pathogenesis. As the main metabolites of intestinal microorganisms, SCFAs play important roles in regulating the balance of intestinal flora, improving intestinal function, anti-inflammation, anti-tumor activity, and regulation of gene expression.

Studies have found that the SCFA content in many chronic diseases, such as obesity, diabetes, and enteritis, is significantly different between the disease and normal groups. At the same time, SCFAs can regulate a variety of neurological diseases including AD through direct or indirect effects. In this study, we aimed to investigate changes in the content of short-chain fatty acids in the feces of mice in each group after drug intervention to determine the potential

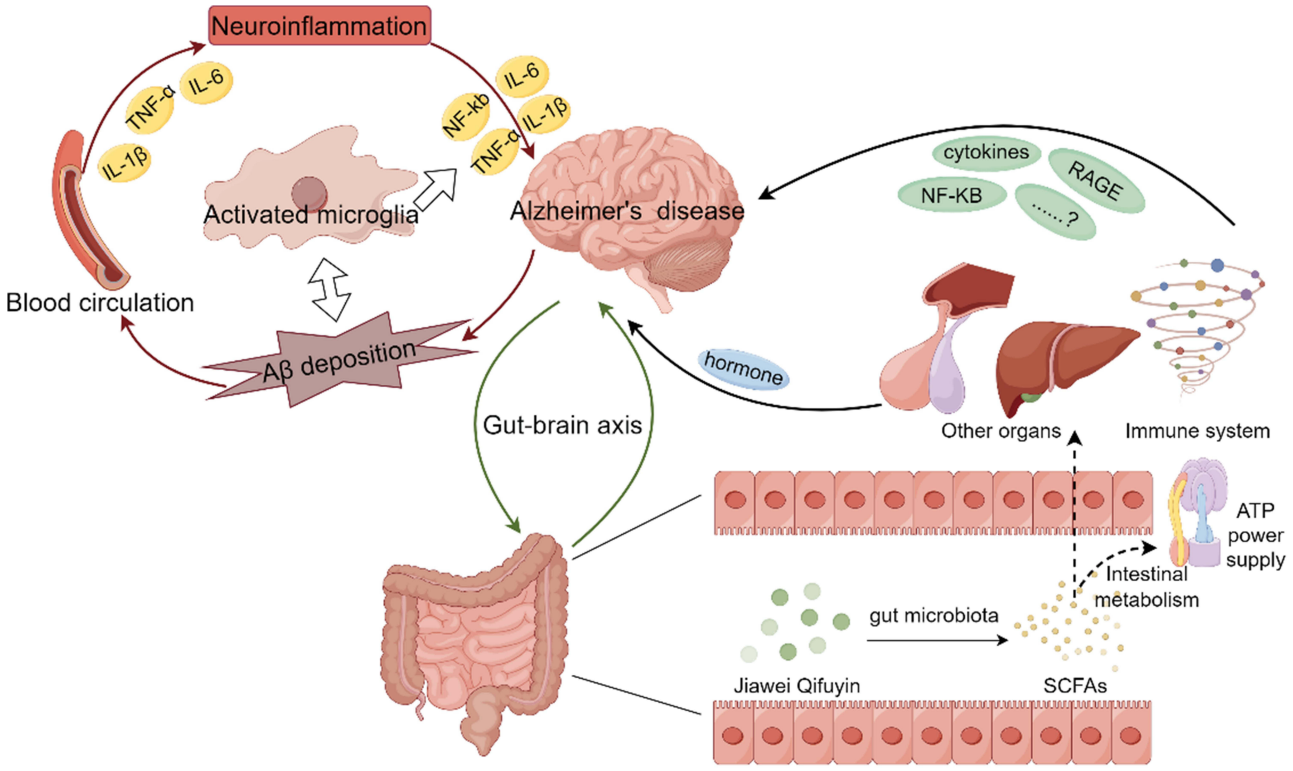

Figure 14 Potential active mechanism of Jiawei Qifuyin against AD.

relationship between them and AD. Acetic acid and butyric acid are the two most abundant SCFAs in the intestine. Acetate exerts neuroprotective effects by upregulating GPR41 and inhibiting the ERK/JNK/NF-κB pathway, reducing neuroinflammatory responses in APP/PS1 mice, and alleviating cognitive impairment in AD mice. Butyrate is a short-chain fatty acid that protects intestinal health.[13] Studies have shown that an increase in butyrate content can not only improve intestinal barrier function and reduce the risk of inflammation, but also help delay aging and cognitive decline.

In this study, we found that after drug intervention, the SCFA content in the feces of each group of mice changed compared to that of the BC group. Acetic acid content in the intestines of mice in the PC, LQ, LMQ, KZ, BZ, and BL intervention groups was significantly higher than that in the BC group. Except for the MMQ intervention group, the intestinal butyric acid content in the drug intervention groups was significantly higher than that in the BC group. Therefore, based on Figure 6A–D and the above experimental results, we found that Jiawei Qifu Yin, sodium butyrate, and Zunyimycin C may improve the cognitive function of AD mice by changing the structure, distribution, function, and metabolism of intestinal flora in AD mice, thereby exerting a neuroprotective effect in AD mice by regulating the gut-brain axis (Figure 14).

Drugs are divided into groups that enter the body of mice and are absorbed through the intestine, which changes the abundance of Bacteroides, Firmicutes, Verrucobacteria, and Epsilon bacteraeota. It can also regulate the metabolic products of SCFAs in intestinal flora.[14] A large amount of SCFAs can reduce the activation of inflammatory bodies and glial cells, mainly acetate, propionate, and butyrate, which can reduce the level of inflammatory factors in the body, protect the blood-brain barrier, and protect the body from inflammation. Intestinal microorganisms can cross the intestinal mucosal barrier and enter the blood, causing the activation of immune cells, such as lymphocytes and macrophages, and the production of cytokines, such as TNF-α, IFN-γ, IL-6, and IL-8, which can cross the blood-brain barrier and lead to neuroinflammation.[15] Lipopolysaccharide (LPS) components of some gram-negative bacterial cell walls can cross the blood-brain barrier, activate microglia and astrocytes, release inflammatory factors such as IL-1, IL-6, and TNF-α, and cause neuroinflammation.[16,17] RAGE receptors on the surface of microglia activate the downstream NF-κB, MAPK, and PI3K-AKT signaling pathways and eventually release inflammatory factors such as IL-1, IL-6, IL-8, and MCP-1, leading to neuroinflammation.[18] Our experimental results showed that intervention with low-dose Qifuyin caused the relative abundance of intestinal flora of APP/PS1 mice to be closest to that of C57 mice, promoted the recovery of intestinal metabolites, promoted the proliferation of immune cells, reduced the expression of inflammatory factors, and improved the cognition of APP/PS1 mice. Butyrate and zunyimycinC also downregulate the expression of pro-inflammatory factors, thereby protecting the brain. Therefore, low-dose Jiawei Qifuyin, butyrate, and zunyimyinC are promising drugs for the treatment of AD neuroinflammation.

Conclusion

In the present study, we delved into the protective efficacy of Jiawei Qifuyin against Alzheimer's disease (AD) through a comprehensive approach that encompassed network pharmacological predictions, in vitro assessments of cell viability, and experiments involving an APP/PS1 transgenic mouse model of AD. Our findings underscored the advanced glycation end products/receptor for advanced glycation end products (AGEs/RAGE) pathway as a pivotal target in the intervention mechanism of Jiawei Qifuyin against AD, thereby laying a solid groundwork for further exploration into its anti-AD mechanisms.

Moreover, Qifuyin was found to exhibit a multifaceted profile of activities, including antioxidant, immunomodulatory, and antineuritic properties. Notably, the combination of Jiawei Qifuyin with ZunyimycinC emerged as a promising strategy to enhance cognitive function in AD mice. This effect appears to be mediated through modulating the intestinal flora's structure, function, and metabolism, which in turn exerts neuroprotection by influencing the gut-brain axis and the interconnected AGE/RAGE/NF-κB signaling pathway.[19] This research thus highlights the potential therapeutic value of Jiawei Qifuyin and ZunyimycinC in ameliorating AD symptoms via a gut microbiota-centric mechanism.

Abbreviations

AD, Alzheimer's disease; Aβ, β-amyloid;APP, amyloid precursor protein; IL-2, Interleukin 2; IL-6, Interleukin 6; IL-1β, Interleukin 1β; IFN-γ, Interferon γ; LPS, Lipopolysaccharide; PI3K, Phosphoinositol 3 kinase; RAGE, recombinant receptor for advanced glycation end products; SCFAs, short-chain fatty acid; TNF-α, Tumor Necrosis Factor-α.

Data Sharing Statement

The datasets used and/or analyzed during the current study are available from the corresponding author upon reasonable request.

Ethics Approval and Consent to Participate

All procedures involving mice strictly followed the guidelines of the National Institutes of Health for the care and use of laboratory animals, and were approved by the Animal Experiment Center of Yan University and the Medical and Biological Research Ethics Committee of Yan'an University (animal license number: SCXK(Su)2021-0013). All animal experiments were performed according to the Guide for the Care and Use of Laboratory Animals.

Acknowledgments

We thank members of the Medical Research Center of Yan'an University School of Medicine and Laboratory of Microbial Drug Innovation and Transformation for technical support and helpful suggestions.

Author Contributions

All authors made a significant contribution to the work reported, whether that is in the conception, study design, execution, acquisition of data, analysis and interpretation, or in all these areas; took part in drafting, revising or critically reviewing the article; gave final approval of the version to be published; have agreed on the journal to which the article has been submitted; and agree to be accountable for all aspects of the work.

Funding

This study was partially supported by the National Nature Science Foundation of China (No. 82060654) and the Shaanxi Provincial Science and Technology Fund (2024JC-YBMS-755).

Disclosure

No conflict of interest between authors.

References

1. Akbarzadeh M, Mihanfar A, Akbarzadeh S, Yousefi B, Majidinia M. Crosstalk between miRNA and PI3K/AKT/mTOR signaling pathway in cancer. *Life Sci*. 2021;285:119984. doi:10.1016/j.lfs.2021.119984
2. Hu J, Wang Q, Wang Y, et al. Polydopamine-based surface modification of hemoglobin particles for stability enhancement of oxygen carriers. *J Colloid Interface Sci*. 2020;571:326–336. doi:10.1016/j.jcis.2020.03.046
3. Kesika P, Suganthy N, Sivamaruthi BS, Chaiyasut C. Role of gut-brain axis, gut microbial composition, and probiotic intervention in Alzheimer's disease. *Life Sci*. 2021;264:118627. doi:10.1016/j.lfs.2020.118627
4. Khan S, Barve KH, Kumar MS. Recent advancements in pathogenesis, diagnostics and treatment of Alzheimer's Disease. *Curr Neuropharmacol*. 2020;18:1106–1125. doi:10.2174/1570159X18666200528142429
5. Leng F, Edison P. Neuroinflammation and microglial activation in Alzheimer disease: where do we go from here? *Nat Rev Neurol*. 2021;17:157–172. doi:10.1038/s41582-020-00435-y
6. Li X, Wei S, Niu S, et al. Network pharmacology prediction and molecular docking-based strategy to explore the potential mechanism of Huanglian Jiedu Decoction against sepsis. *Comput Biol Med*. 2022;144:105389. doi:10.1016/j.compbiomed.2022.105389
7. Liu Q, Xie T, Xi Y, et al. Sesamol attenuates amyloid peptide accumulation and cognitive deficits in APP/PS1 mice: the mediating role of the gut-brain axis. *J Agric Food Chem*. 2021;69:12717–12729. doi:10.1021/acs.jafc.1c04687
8. Liu S, Gao J, Zhu M, Liu K, Zhang H-L. Gut microbiota and dysbiosis in Alzheimer's disease: implications for pathogenesis and treatment. *Mol Neurobiol*. 2020;57:5026–5043. doi:10.1007/s12035-020-02073-3
9. Ma C, Hong F, Yang S. Amyloidosis in Alzheimer's disease: pathogeny, etiology, and related therapeutic directions. *Mol*. 2022;27:1210. doi:10.3390/molecules27041210
10. Ozben T, Ozben S. Neuro-inflammation and anti-inflammatory treatment options for Alzheimer's disease. *Clin Biochem*. 2019;72:87–89. doi:10.1016/j.clinbiochem.2019.04.001
11. Revathidevi S, Munirajan AK. Akt in cancer: mediator and more. *Semin Cancer Biol*. 2019;59:80–91. doi:10.1016/j.semcancer.2019.06.002
12. Singh D. Astrocytic and microglial cells as the modulators of neuroinflammation in Alzheimer's disease. *J Neuroinflammation*. 2022;19:206. doi:10.1186/s12974-022-02565-0
13. Wang C, Zheng D, Weng F, Jin Y, He L. Sodium butyrate ameliorates the cognitive impairment of Alzheimer's disease by regulating the metabolism of astrocytes. *Psychopharmacology*. 2022;239:215–227. doi:10.1007/s00213-021-06025-0
14. Wang M, Pan W, Xu Y, Zhang J, Wan J, Jiang H. Microglia-mediated neuroinflammation: a potential target for the treatment of cardiovascular diseases. *J Inflamm Res*. 2022;15:3083–3094. doi:10.2147/JIR.S350109

15. Wang X, Li Z, Sun R, et al. Zunyimycin C enhances immunity and improves cognitive impairment and its mechanism. *Front Cell Infect Microbiol*. 2022;12:1081243. doi:10.3389/fcimb.2022.1081243
16. Wang X, Yu S, Hu J-P, et al. Streptozotocin-induced diabetes increases amyloid plaque deposition in AD transgenic mice through modulating AGEs/RAGE/NF-κB pathway. *Int J Neurosci*. 2014;124:601–608. doi:10.3109/00207454.2013.866110
17. Xie Y, Shi X, Sheng K, et al. PI3K/Akt signaling transduction pathway, erythropoiesis and glycolysis in hypoxia (Review). *Mol Med Rep*. 2019;19:783–791. doi:10.3892/mmr.2018.9713
18. Zhang W-J, Luo C, Huang C, Pu F-Q, Zhu J-F, Zhu Z-M. PI3K/Akt/GSK-3β signal pathway is involved in P2X7 receptor-induced proliferation and EMT of colorectal cancer cells. *Eur J Pharmacol*. 2021;899:174041. doi:10.1016/j.ejphar.2021.174041
19. Zhu Z, Ma X, Wu J, et al. Altered gut microbiota and its clinical relevance in mild cognitive impairment and Alzheimer's disease: Shanghai aging study and Shanghai Memory Study. *Nutrients*. 2022;14:3959. doi:10.3390/nu14193959